Tanshinone IIA confers protection against myocardial ischemia/reperfusion injury by inhibiting ferroptosis and apoptosis via VDAC1

TIE HU[1,2*], HUA-XI ZOU[1,2*], SHU-YU LE[1,2*], YA-RU WANG[1], YA-MEI QIAO[1], YONG YUAN[1], JI-CHUN LIU[2], SONG-QING LAI[1] and HUANG HUANG[1]

[1]Institute of Cardiovascular Surgical Diseases, Jiangxi Academy of Clinical Medical Sciences, The First Affiliated Hospital of Nanchang University; [2]Department of Cardiovascular Surgery, The Second Affiliated Hospital of Nanchang University, Nanchang, Jiangxi 330006, P.R. China

Received June 7, 2023; Accepted September 6, 2023

DOI: 10.3892/ijmm.2023.5312

Abstract. Tanshinone IIA (TSN) extracted from danshen (*Salvia miltiorrhiza*) could protect cardiomyocytes against myocardial ischemia/reperfusion injury (IRI), however the underlying molecular mechanisms of action remain unclear. The aim of the present study was to identify the protective effects of TSN and its mechanisms of action through *in vitro* studies. An anoxia/reoxygenation (A/R) injury model was established using H9c2 cells to simulate myocardial IRI *in vitro*. Before A/R, H9c2 cardiomyoblasts were pretreated with 8 μM TSN or 10 μM ferrostatin-1 (Fer-1) or erastin. The cell counting kit 8 (CCK-8) and lactate dehydrogenase (LDH) assay kit were used to detect the cell viability and cytotoxicity. The levels of total iron, glutathione (GSH), glutathione disulfide (GSSG), malondialdehyde (MDA), ferrous iron, caspase-3 activity, and reactive oxygen species (ROS) were assessed using commercial kit. The levels of mitochondrial membrane potential (MMP), lipid ROS, cell apoptosis, and mitochondrial permeability transition pore (mPTP) opening were detected by flow cytometry. Transmission electron microscopy (TEM) was used to observed the mitochondrial damage. Protein levels were detected by western blot analysis. The interaction between TSN and voltage-dependent anion channel 1 (VDAC1) was evaluated by molecular docking simulation. The results showed that pretreatment with TSN and Fer-1 significantly decreased cell viability, glutathione peroxidase 4 (GPX4) protein and GSH expression and GSH/GSSG ratio and inhibited upregulation of LDH activity, prostaglandin endoperoxide synthase 2 and VDAC1 protein expression, ROS levels, mitochondrial injury and GSSG induced by A/R. TSN also effectively inhibited the damaging effects of erastin treatment. Additionally, TSN increased MMP and Bcl-2/Bax ratio, while decreasing levels of apoptotic cells, activating Caspase-3 and closing the mPTP. These effects were blocked by VDAC1 overexpression and the results of molecular docking simulation studies revealed a direct interaction between TSN and VDAC1. In conclusion, TSN pretreatment effectively attenuated H9c2 cardiomyocyte damage in an A/R injury model and VDAC1-mediated ferroptosis and apoptosis served a vital role in the protective effects of TSN.

Correspondence to: Dr Huang Huang or Dr Song-Qing Lai, Institute of Cardiovascular Surgical Diseases, Jiangxi Academy of Clinical Medical Sciences, The First Affiliated Hospital of Nanchang University, 17 Yongwai Road, Nanchang, Jiangxi 330006, P.R. China
E-mail: jack19871212@hotmail.com
E-mail: ndyfy03743@email.ncu.edu.cn

[*]Contributed equally

Key words: tanshinone IIA, ischemia/reperfusion injury, voltage-dependent anion channel 1, apoptosis, ferroptosis

Introduction

Acute myocardial infarction (AMI) is a key cause of high mortality in various types of cardiovascular disease (1,2). Although timely reperfusion therapy to salvage cardiomyocytes effectively improves patient outcomes, many studies have demonstrated that reperfusion also results in additional myocardial damage and dysfunction of tissue, resulting in myocardial ischemia/reperfusion injury (IRI) (3,4). The pathophysiological processes underlying development of IRI are complicated and involve numerous pathogenic factors, including inflammatory responses and excess accumulation of reactive oxygen species (ROS) (5). Novel treatments are required to improve clinical prognosis following AMI and IRI. Traditional Chinese medicine (TCM) has shown protective effects against cardiovascular disease, type 2 diabetes mellitus, and malaria (6). Therefore, the protective role of TCM for IRI needs further research.

As a TCM, Danshen (*Salvia miltiorrhiza*) has been applied to prevent tissue damage and organ dysfunction induced by cardiovascular disease, including MI and arrhythmia (7). Tanshinone IIA (TSN) is extracted from the rhizome of Danshen and serves an important role as an anti-inflammatory,

antioxidant, and antithrombotic agent in vascular smooth muscle cells, improving AMI (8-10). Additionally, TSN confers protection against IRI *in vivo*, mediated by the PI3K/Akt/mTOR signaling pathway. The infarct size and apoptosis rate of cardiac cells is significantly reduced in an IRI model following pretreatment with TSN (11). To the best of our knowledge, previous studies have only focused on biomarkers of apoptosis and oxidative stress; the underlying molecular mechanisms of TSN and involvement of ferroptosis are unknown.

Apoptosis has been reported as a primary form of cell death caused by IRI (12). In several studies, it has been reported that ferroptosis also participates in the development of IRI (1,13). As a novel form of regulated cell death, ferroptosis is an iron- and lipotoxicity-dependent type of programmed cell death, which is primarily caused by excessive generation of intracellular ROS (14,15). Ferroptosis and apoptosis are activated by the upregulation of voltage-dependent anion channel 1 (VDAC1) in IRI (16,17). As a key component of the outer membrane of mitochondria, VDAC1 participates in the transportation of metabolites, nucleotides and ions (16). Moreover, previous studies have shown that expression of VDAC1 is upregulated and indicates more severe myocardial damage after anoxia/reoxygenation (A/R) treatment (18,20).

Therefore, the present study aimed to explore whether TSN could induce myocardial protection by inhibiting ferroptosis and apoptosis and whether the protective effects of TSN are regulated by VDAC1.

Materials and methods

Materials and chemicals. TSN (purity: 98%) was obtained from the National Institutes for Food and Drug Control (Beijing, China). Adenovirus pAd/VDAC1 and pAd/negative control (NC) were purchased from Suzhou GenePharma Co., Ltd. Ferrostatin-1 (Fer-1, ferroptosis inhibitor), erastin (ferroptosis inducer), Z-Val-Ala-DL-Asp-fluoromethylketone (Z-VAD, apoptosis inhibitor) and N-acetylcysteine (NAC; ROS inhibitor) were obtained from MedChemExpress. The primary antibodies against glutathione peroxidase 4 (GPX4), Bcl-2 and Bax were obtained from Chengdu Zhengneng Biotechnology Co., Ltd. and VDAC1, prostaglandin endoperoxide synthase 2 (PTGS2) and β-actin were obtained from Proteintech Group, Inc. Goat anti-mouse and goat anti-rabbit secondary antibodies were obtained from Beyotime Institute of Biotechnology.

H9c2 cardiomyocyte culture and construction of A/R injury model. Rat H9c2 cardiomyocytes, purchased from Cell Bank/Stem Cell Bank (Beijing, China), were cultured as a monolayer in high-glucose Dulbecco's modified Eagle's medium (H-DMEM; HyClone, Cytiva) with 10% fetal bovine serum (FBS; Gibco, Thermo Fisher Scientific, Inc.) at 37˚C under normal conditions (95% humidity, 21% O_2 and 5% CO_2), as described by Pooja *et al* (19).

As described in previous studies (20,21), the cell A/R liquid method was applied to establish an *in vitro* A/R model. H9c2 cells were incubated in anoxia medium ($CaCl_2$ 1.0, HEPES 20.0, KCl 10.0, $MgSO_4$ 1.2, NaCl 98.5, NaH_2PO_4 0.9, $NaHCO_3$ 6.0 and sodium lactate 40.0 mM, pH 6.8) and 95% N_2 and 5% CO_2 at 37˚C for 3 h. Reoxygenation medium ($CaCl_2$ 1.0, glucose 5.5, HEPES 20.0, KCl 5.0, $MgSO_4$ 1.2 mM, NaCl 129.5, NaH_2PO_4 0.9 and $NaHCO_3$ 20.0 mM, pH 7.4) was used to simulate IRI and cells were incubated under 95% O_2 and 5% CO_2 at 37˚C for 2 h.

Adenovirus preparation and transduction. Adenoviral vector CMV-ADV6 (Suzhou GenePharma Co., Ltd.) was digested using *Eco*RI and *Bam*HI. The open reading frame sequence of rat VDAC1 gene [NCBI (National Center for Biotechnology Information) reference sequence NM_031353.1] (22) was amplified using PCR using Power SYBR Green PCR MasterMix (Thermo Fisher Scientific, Inc.) and used to establish CMV-ADV6-VDAC1 by linearizing and inserting into the CMV-ADV6 (Suzhou GenePharma Co., Ltd.). PCR process involved initial denaturation at 95˚C for 10 min, followed by thermocycling 95˚C for 15 sec, and 60˚C for 1 min, repeated 40 cycles. To acquire positive clones, the recombinant plasmid was tranduced into DH5α-competent cells (Tiangen) at 37˚C for 16 h and the positive clone was confirmed by liquid sequencing. Plasmid Midi Preparation kit (Beijing CW Biotech Co., Ltd.) was used to prepare the recombinant plasmids following the manufacturer's instructions. Next, CMV-ADV6-VDAC1 was transduced into 293 cells (ATCC, cat. no. CRL-1573) using RNAi-mate (Suzhou GenePharma Co., Ltd.) and a 2nd generation system under 95% O_2 and 5% CO_2 at 37˚C for 6 h (quantity of adenovirus plasmid used for transfection is 10 μg and the ratio used for adenovirus, packaging and envelope plasmids is 1:3:4). Finally, the supernatant was collected after centrifugation at 7,000 x g for 5 min at 4˚C following virus amplification and the generated adenoviral vectors were amplified until the viral titer reached $1x10^9$ plaque-forming units (PFU)/ml.

pAd/VDAC1 or pAd/NC were transduced into H9c2 cardiomyocytes cultured in fresh H-DMEM supplemented with 10% FBS (multiplicity of infection, 100) under 95% O_2 and 5% CO_2 at 37˚C for 48 h. H9c2 cells not transduced with adenovirus were used as Control. Then, subsequent experiments were conducted.

H9c2 cardiomyocyte treatment. H9c2 cells were randomly divided into the following groups: i) Control, H9c2 cardiomyocytes cultured under normal conditions; ii) A/R, H9c2 cardiomyocytes exposed to A/R; iii) TSN, H9c2 cardiomyocytes pretreated with TSN (1, 2, 4, 8, 16 and 32 μM) at 37˚C for 48 h; iv) TSN + A/R, H9c2 cardiomyocytes pretreated with TSN (1, 2, 4, 8, 16 and 32 μM) at 37˚C for 48 h before A/R injury; v) 8 μM TSN + A/R, H9c2 cardiomyocytes pretreated with 8 μM TSN at 37˚C for 48 h before A/R injury; vi) Fer-1 + A/R, H9c2 cardiomyocytes pretreated with 10 μM Fer-1 at 37˚C for 2 h before A/R; vii) erastin, H9c2 cardiomyocytes treated with 10 μM Erastin at 37˚C for 24 h; viii) erastin + TSN, H9c2 cardiomyocytes pretreated with 8 μM TSN for 48 h before erastin treatment; ix) Z-VAD + A/R, H9c2 cells pretreated with 40 μM Z-VAD at 37˚C for 24 h before A/R; x) NAC + A/R, H9c2 cardiomyocytes pretreated with 6 mM NAC at 37˚C for 6 h before A/R injury; xi) pAd/VDAC1 + TSN + A/R, H9c2 cardiomyocytes transfected with pAd/VDAC1 and pretreated with 8 μM TSN for 48 h before A/R and xii) pAd/NC + TSN + A/R, H9c2 cardiomyocytes transfected with pAd/NC and pretreated with 8 μM TSN for 48 h before A/R.

Assessment of cell viability. Cell viability was determined by colorimetric assay using Cell Counting Kit-8 assay (CCK-8; GlpBio Technology). Briefly, H9c2 cardiomyocytes were seeded in 96-well plates at a density of $1x10^4$ cells/well, and incubated with 10 μl CCK-8 reagent/100 μl H-DMEM (HyClone, Cytiva) added with 10% FBS (Gibco, Thermo Fisher Scientific, Inc.) for 1 h at 37˚C. Finally, the absorbance was measured at 450 nm using a microplate reader (Thermo Fisher Scientific, Inc.).

Assessment of cytotoxicity. Following different treatments, the cell culture medium was harvested, and the lactate dehydrogenase (LDH) levels were determined by LDH assay kits (Beyotime Institute of Biotechnology, cat. no. #C0016) following the manufacturer's instructions. Furthermore, cytotoxicity was calculated by dividing absorbance of the experimental wells by 100%.

Measurement of malondialdehyde (MDA), total iron and glutathione (GSH)/glutathione disulfide (GSSG) levels. Following treatment, H9c2 cardiomyocytes from each group were digested with 0.25% trypsin, washed twice with phosphate-buffered saline (PBS) and lysed by ultrasound (20 kHz for 3 min) to obtain cell homogenates. The supernatant was obtained after centrifugation at 12,000 x g for 15 min at 4˚C. The supernatant was used to determine the intracellular levels of MDA, total iron, GSH and glutathione disulfide (GSSG) and the GSH/GSSG ratio using MDA assay kit (Beyotime Institute of Biotechnology, cat. no. #S0131S), total iron assay kit [Applygen (https://www.applygen.com/), cat. no. #E1042] and GSH and GSSG assay kits (Beyotime Institute of Biotechnology, cat. no. #S0053), according to the manufacturer's instructions.

Caspase-3 activity assay. Following treatment, the activity of caspase-3 was determined using caspase-3 activity assay kit (Beyotime Institute of Biotechnology, cat. no. #C1115) according to the manufacturer's instruction. In brief, 40 reaction buffer, 50 cell homogenate extracted from each group and 10 μl caspase-3 substrates were added to a 96-well plate and incubated for 2 h at 37˚C. Next, absorbance was measured using a microplate reader at 405 nm. Finally, the Bradford method was used to assess the protein concentration in each group (23).

Determination of intracellular ROS. The levels of intracellular ROS were determined by an Olympus IX 73 microscope (Olympus Corporation) using DCFH-DA (Beyotime Institute of Biotechnology, cat. no. S0033S). DCFH-DA enters the cell and can be lysed into DCFH by esterases that cannot cross the cell membrane and be oxidized by intracellular ROS into fluorescent DCF (24). Briefly, DCFH-DA (10 μM) dye was added to cells and incubated for 20 min in the dark at 37˚C. Next, levels of intracellular ROS were detected using the fluorescence microscope (magnification, x200).

Assessment of intracellular ferrous iron levels. The intracellular Fe^{2+} level was measured using FerroOrange (Dojindo Laboratories, Inc.) based on the manufacturer's instructions. Briefly, treated H9c2 cardiomyocytes were treated with 1 μM FerroOrange and 0.5 μg/ml Hoechst 33342 (Beyotime Institute of Biotechnology) at 37˚C for 30 min in the dark. Excess FerroOrange and Hoechst 33342 were removed by washing twice with PBS. Finally, the fluorescence microscope (magnification, x200) was used to assess the levels of ferrous iron.

Mitochondrial membrane potential (MMP) assay. MMP was determined using the JC-1 MMP Detection kit (BestBio) following the manufacturer's instructions. Briefly, following treatments, H9c2 cells were collected and incubated with JC-1 and quenching agent for 30 min at 37˚C in the dark, washed twice with PBS and the levels of MMP were measured using a Cytomics FC500 flow cytometer [Beckman Coulter, Inc.; 530/580 and 485/530 nm] (analyte detector is Annexin V and PI; the analyte reporter is FITC and PE). The red (JC-1 aggregates) to green (JC-1 monomers) fluorescence intensity ratio of the cells reflects the levels of MMP. NovoExpress (v.6.2; Agilent Technologies, Inc.) was used to analyze the flow cytometry data.

Mitochondrial permeability transition pore (mPTP) opening assay. mPTPs were assessed by BBcellProbe M61 mPTP Detection kit (BestBio). In brief, following treatment, H9c2 cardiomyocytes were collected and cultured with BBcellProbe M61 and a quenching agent for 15 min at 37˚C in the dark, washed twice with PBS and the levels of mPTP were determined using a Cytomics FC500 flow cytometer [excitation (Ex), 488; emission (Em), 558 nm] (The analyte detector is Annexin V; the analyte reporter is FITC). The green fluorescence intensity of BBcellProbe M61 probe [(Ex), 495 nm; (Em), 515 nm] labelled cells represented the levels of mPTP opening. NovoExpress (v.6.2; Agilent Technologies, Inc.) was used to analyze the flow cytometry data.

Apoptosis assay. Cell apoptosis was assayed using the Annexin V-FITC Apoptosis Detection kit (BestBio). In brief, following treatment, H9c2 cardiomyocytes were collected and resuspended in 1X Annexin V binding buffer at a cell density of $1x10^6$ cells/ml. The cell suspension was incubated with 5 Annexin V-FITC and 10 μl PI at 4˚C for 20 min in the dark and detected using a Cytomics FC500 flow cytometer (Ex, 488 nm; Em, 578 nm). Q1 quadrant represented necrotic cells and Q4 quadrant represented live cells. The total apoptosis rate was calculated as the sum of Q2 (late apoptotic cells) and Q3 (early apoptotic cells). NovoExpress (v.6.2; Agilent Technologies, Inc.) was used to analyze data.

Lipid ROS assay. The levels of intracellular lipid ROS were measured using a Cytomics FC500 flow cytometer (analyte detector is Annexin V and PI; the analyte reporter is FITC and PE) with C11-BODIPY581/591 (GlpBio Technology). Briefly, treated H9c2 cardiomyocytes were gathered and incubated with 10 μM C11-BODIPY581/591 in the dark for 30 min at 37˚C and washed twice with PBS. The cells were resuspended in PBS containing 10% FBS. The shift of fluorescence emission peak from ~590 to ~510 nm reflects the increase in lipid ROS levels. NovoExpress (v.6.2; Agilent Technologies, Inc.) was used to analyze the flow cytometry data.

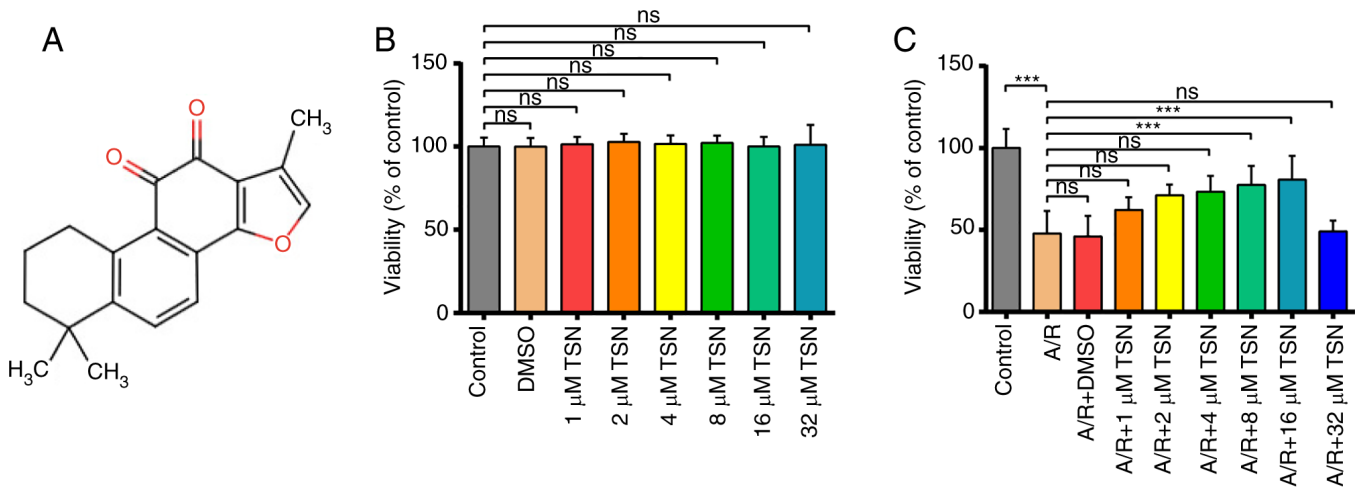

Figure 1. TSN protects H9c2 cardiomyocytes against A/R injury. (A) Chemical structure of TSN. (B) CCK-8 detection of cell viability following TSN treatment. (C) CCK-8 detection of viability of A/R-induced cells following treatment with TSN. Data are expressed as the mean ± SD (n=3). ***P<0.05, TSN, Tanshinone IIA; A/R, Anoxia/reoxygenation; CCK, Cell Counting Kit; ns, not significant.

Mitochondrial ultrastructural assessment. Following the different treatments, H9c2 cells were rapidly gathered and incubated in 2% glutaraldehyde for 2 h. Then, the cells were observed by transmission electron microscopy after washing, dehydration, embedding in Epon 812, sectioning (60 nm), and stained with 2% uranyl acetate and 2.6% lead citrate for 8 min at 37˚C. Additionally, the Flameng score method was applied to determine the mitochondrial ultrastructural injury (25).

Western blot analysis. Following treatment, total cell lysates obtained using radioimmunoprecipitation assay lysis buffer (Beyotime Institute of Biotechnology) with 1% phenylmethylsulfonyl fluoride, incubated at 4˚C for 15 min and the protein concentration was quantified using bicinchoninic acid protein assay kit (Beyotime Institute of Biotechnology). An equal amount of total protein (40 μg/lane) in each sample was separated by 10% sodium dodecyl sulfate-polyacrylamide gel electrophoresis, transferred to polyvinylidene fluoride membranes and blocked with 5% non-fat dry milk in Tris-buffered saline with 0.1% Tween-20 buffer at room temperature for 2 h. Subsequently, membranes were incubated with primary antibodies against PTGS2 (ProteinTech Group, Inc.; cat. no. #12375-1-AP; 1:1,000), VDAC1 (ProteinTech Group, Inc.; cat. no. #55259-1-AP; 1:1,000), GPX4 (ZENBIO; cat. no. #381958; 1:1,000), Bcl-2 (ZENBIO; cat. no. #250412; 1:1,000), Bax (ZENBIO; cat. no. #380709; 1:1,000) and β-actin (ProteinTech Group, Inc.; cat. no. #20536-1-AP; 1:1,000) at 4˚C overnight in a shaker. Then, the PVDF membranes were washed three times for 10 min and incubated with secondary HRP-conjugated antibodies (Beyotime Institute of Biotechnology, cat. no. #A0208; 1:1,000) for 2 h at 25˚C. Finally, an ultra-high-sensitivity ECL kit (Beyotime Institute of Biotechnology) was used to visualize protein bands. The signal intensities of bands were quantified using ImageJ 1.8.0 (National Institutes of Health).

Molecular docking simulation. The molecular docking simulation was performed using Discovery Studio 4.5 software (26). The three-dimensional structure of VDAC1 for molecular docking was obtained from AlphaFold database (UniProt ID: P21796) (27) and the structure of TSN was obtained from PubChem (PubChem CID: 164676) (28). TSN was docked into VDAC1 using LibDock mode in Discovery Studio 4.5 software with parameters selected by a default procedure. Thus, molecular docking scores was calculated using LibDock custom scoring function to evaluate the binding affinity between TSN and VDAC1.

Statistical analysis. Statistical analyses were performed using GraphPad Prism 8.0 (Dotmatics). All experiments were repeated 3 times and the data are expressed as the mean ± standard deviation. Three or more groups were compared by one-way analysis of variance followed by Dunnett's or Tukey's post hoc multiple comparisons test. P≤0.05 was considered to indicate a statistically significant difference.

Results

TSN protects H9c2 cardiomyocytes against A/R injury. The chemical structure of TSN is presented in Fig. 1A. CCK-8 assay was used to measure the viability of H9c2 cardiomyocytes following pretreatment with different concentrations of TSN (0, 1, 2, 4, 8, 16 and 32 μM) and A/R injury. After culturing H9c2 cardiomyocytes with TSN at different concentrations, there was no difference in the viability of H9c2 cells compared with Control group (Fig. 1B). Additionally, A/R injury significantly decreased the cell viability, which was increased significantly after treatment with 8 and 16 μM TSN before A/R. Based on the principle of drug dosage selection (29), 16 μM was considered the limiting level for safe drug concentrations. By contrast, 8 μM TSN optimally enhanced viability of A/R-induced H9c2 cardiomyocytes (Fig. 1C).

TSN alleviates ferroptosis of A/R-induced H9c2 cardiomyocytes via downregulation of VDAC1. TSN at a concentration of 8 μM was selected for subsequent experiments. Pretreatment with TSN and Fer-1 before A/R injury significantly increased the cell viability that was decreased by A/R injury and

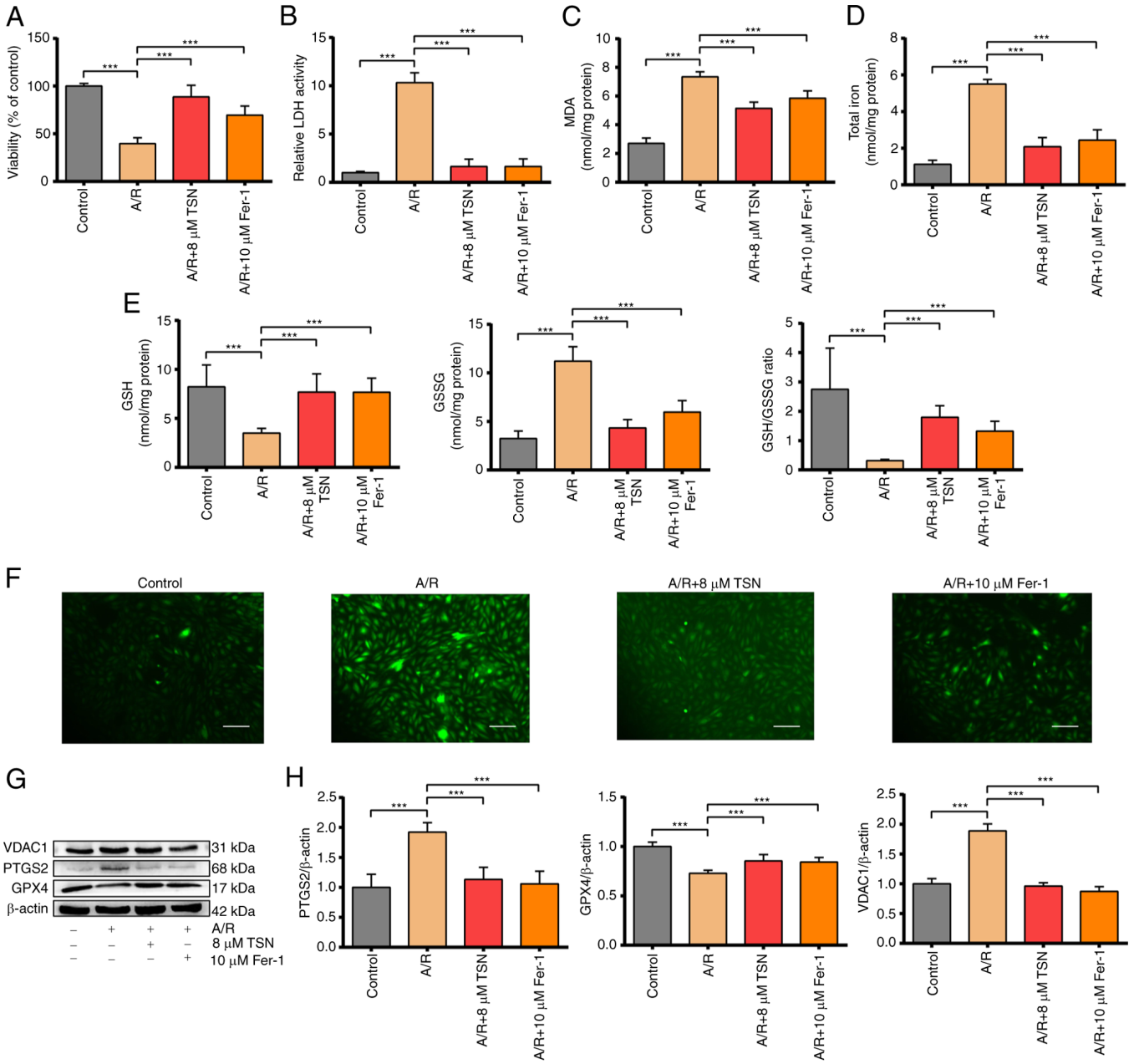

Figure 2. TSN alleviates ferroptosis of A/R-induced H9c2 cardiomyocytes via downregulation of VDAC1. (A) Cell Counting Kit-8 detection of viability in A/R-induced cells following TSN or Fer-1 pretreatment. (B) LDH, (C) MDA, (D) total iron, (E) GSH, GSSG, GSH/GSSG and (F) ROS were determined by quantitative kits in A/R-induced cells following TSN or Fer-1 treatment (magnification, x200; scale bar, 50 μm). (G) Expression of (H) ferroptosis-related proteins and VDAC1 were detected by western blot analysis in A/R-induced cells following TSN or Fer-1 pretreatment. Data are expressed as the mean ± SD (n=3). ***P<0.05. TSN, Tanshinone IIA; A/R, Anoxia/reoxygenation; VDAC1, Voltage-dependent anion channel 1; Fer-1, ferrostatin-1; LDH, lactate dehydrogenase; MDA, malondialdehyde; GSH, Glutathione; GSSG, Glutathione disulfide; ROS, reactive oxygen species; PTGS2, Prostaglandin endoperoxide synthase 2; GPX, Glutathione peroxidase 4.

decreased levels of LDH activity that were increased significantly by A/R injury, suggesting pretreatment with 8 μM TSN and 10 μM Fer-1 could effectively protect H9c2 cardiomyocytes against A/R injury (Fig. 2A and B). It has previously been reported that iron overload and abnormal lipid metabolism are key features of ferroptosis (30,31). The total iron content and products of lipid peroxidation such as MDA were significantly increased in A/R group and reduced by TSN and Fer-1 pretreatment (Fig. 2C and D). In addition, as an important part of the non-enzymatic antioxidant system, GSH is used by glutathione peroxidase 4 (GPX4) to remove excess lipid metabolites (32). A/R injury significantly increased the levels of GSSG and decreased the levels of GSH and the GSH/GSSG ratio in H9c2 cardiomyocytes, while pretreatment with TSN and Fer-1 reversed these changes (Fig. 2E). Accumulation of excess ROS not only damages lipids and triggers abnormal lipid metabolism leading to ferroptosis but is also the critical outcome of ferroptosis (5). Pretreatment with TSN and Fer-1 significantly attenuated the increase in intracellular ROS induced by A/R (Fig. 2F). Expression of PTGS2 and GPX4, positive/negative molecular markers of ferroptosis, was measured in cell lysate (33). Following A/R treatment, PTGS2

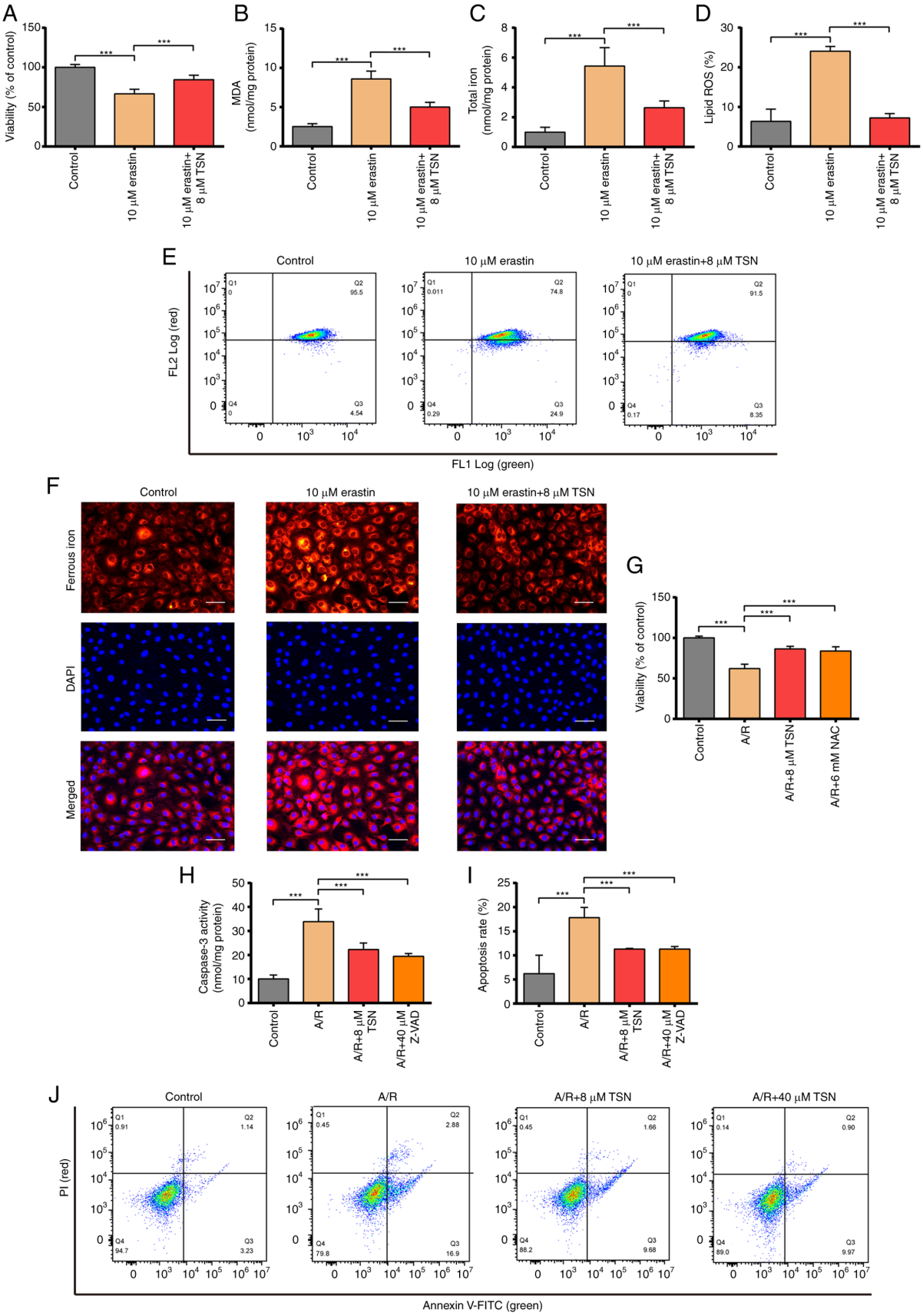

Figure 3. TSN attenuates ferroptosis of erastin-induced H9c2 cells and inhibits apoptosis of A/R-induced H9c2 cardiomyocytes. (A) CCK-8 detection of viability in H9c2 cells following erastin or TSN treatment. (B) MDA, (C) total iron, (D) lipid ROS were determined by quantitative kits in H9c2 cells after erastin or TSN treatment. Quantitative analysis for (E) the levels of intracellular lipid ROS. (F) Ferrous iron was measured by quantitative kits in H9c2 cells after erastin or TSN treatment (magnification, x200; scale bar, 50 μm). (G) CCK-8 detected viability in A/R-induced cells after TSN or NAC pretreatment. (H) Caspase-3 activity was measured using a Caspase-3 quantitative kit in A/R-induced cells following TSN or Z-VAD treatment. (I) Apoptotic rate was (J) measured by Annexin V-FITC/PI detected by flow cytometry. Data are expressed as the mean ± SD (n=3). ***P<0.05. TSN, tanshinone IIA; A/R, Anoxia/reoxygenation; CCK, Cell Counting Kit; MDA, malondialdehyde; ROS, reactive oxygen species; NAC, N-acetylcysteine; Z-VAD, Z-Val-Ala-DL-Asp-fluoromethylketone.

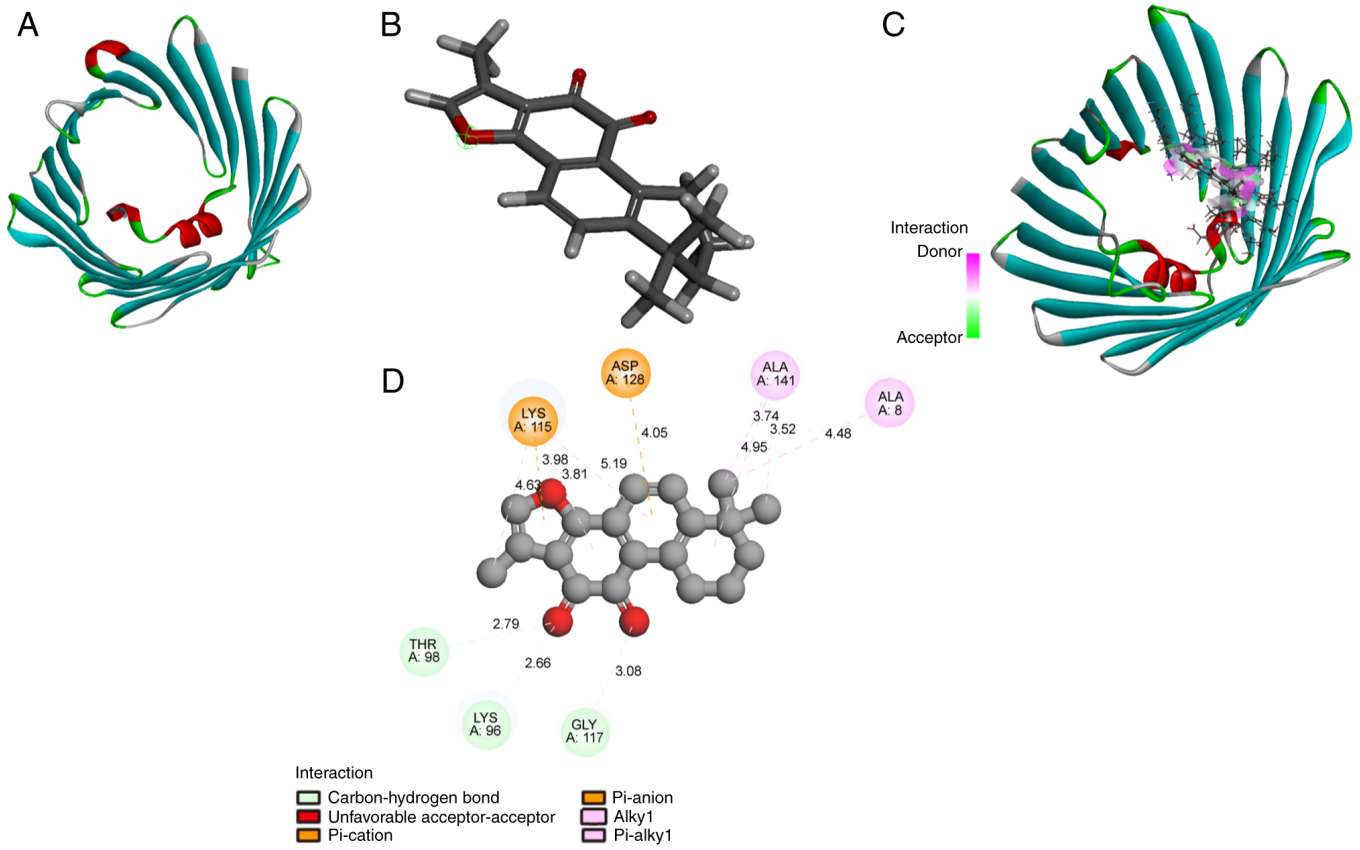

Figure 4. TSN binds to VDAC1. (A) Chemical structure of TSN. (B) Molecular structure of VDAC1. (C) 3D and (D) 2D diagram of the interaction between TSN and VDAC1. TSN, Tanshinone IIA; VDAC1, Voltage-dependent anion channel 1.

expression was significantly increased and GPX4 expression was decreased; these effects were reversed by pretreatment with TSN and Fer-1 (Fig. 2G and H). Furthermore, VDAC1 expression in H9c2 cardiomyocytes in A/R group increased significantly compared with that in control group and was decreased in H9c2 cardiomyocytes pretreated with TSN and Fer-1 (Fig. 2G and H). Together, the results showed that VDAC1 was involved in ferroptosis during A/R injury and may mediate the protective effect of TSN against ferroptosis in A/R injury.

TSN attenuates erastin-induced ferroptosis and inhibits apoptosis of A/R-induced H9c2 cells. To confirm that TSN alleviates A/R injury by inhibiting ferroptosis and apoptosis, the present study explored the protective role of TSN on erastin-induced H9c2 cell injury. Viability of erastin-induced H9c2 cardiomyocytes was significantly decreased and levels of lipid ROS, ferrous iron, MDA and total iron were significantly increased in erastin group (Fig. 3A-F). Pretreatment with TSN effectively reversed the harmful effects of erastin (Fig. 3A-F). Based on the main biological signs (lipid peroxidation and iron overload) of ferroptosis, TSN served a biological role in attenuating ferroptosis and TSN alleviated A/R injury by inhibiting ferroptosis (Figs. 2 and 3A-F). Excess ROS generation has been reported to play a key role in the pathological process of IRI and triggers multiple forms of regulated cell death, including apoptosis and ferroptosis (34,35). Therefore, the protective effect of NAC on A/R injury was investigated. A/R treatment significantly reduced the cell viability, while NAC or TSN pretreatment effectively abolished the damaging effects of A/R (Fig. 3G).

To validate that the protective effects of TSN on A/R-induced H9c2 cell injury were partly due to the inhibition of apoptosis, the present study elucidated the protective effect of TSN on A/R-induced apoptosis. TSN and Z-VAD pretreatment significantly inhibited apoptosis of H9c2 cardiomyocytes and significantly decreased the increased caspase3 activity in H9c2 cardiomyocytes caused by A/R (Fig. 3H-J).

TSN binds to VDAC1. Molecular docking is widely used to assay potential bioactivity of compounds (36,37). Computational modeling was performed to investigate the direct interaction between TSN and VDAC1. The structures of TSN and VDAC1 are shown in Fig. 4A and B, respectively. Molecular docking of TSN-VDAC1 was performed using LibDock module of Discovery Studio 4.5 software. TSN strongly bound to residues Thr-98, Lys-96, and Gly-117 by hydrogen bonds (Fig. 4C and D) with a high combination score (93.0347). Therefore, VDAC1 was a possible potential target of TSN.

TSN inhibits ferroptosis of A/R-induced H9c2 cardiomyocytes by downregulating VDAC1. VDAC1 is an important ferroptosis regulator in IRI (16). Therefore, the present study aimed to verify the role of TSN in the modulation of the VDAC1 levels. After confirming successful transduction of pAd/VDAC1 and pAd/NC into H9c2 cells (Fig. S1). A/R significantly

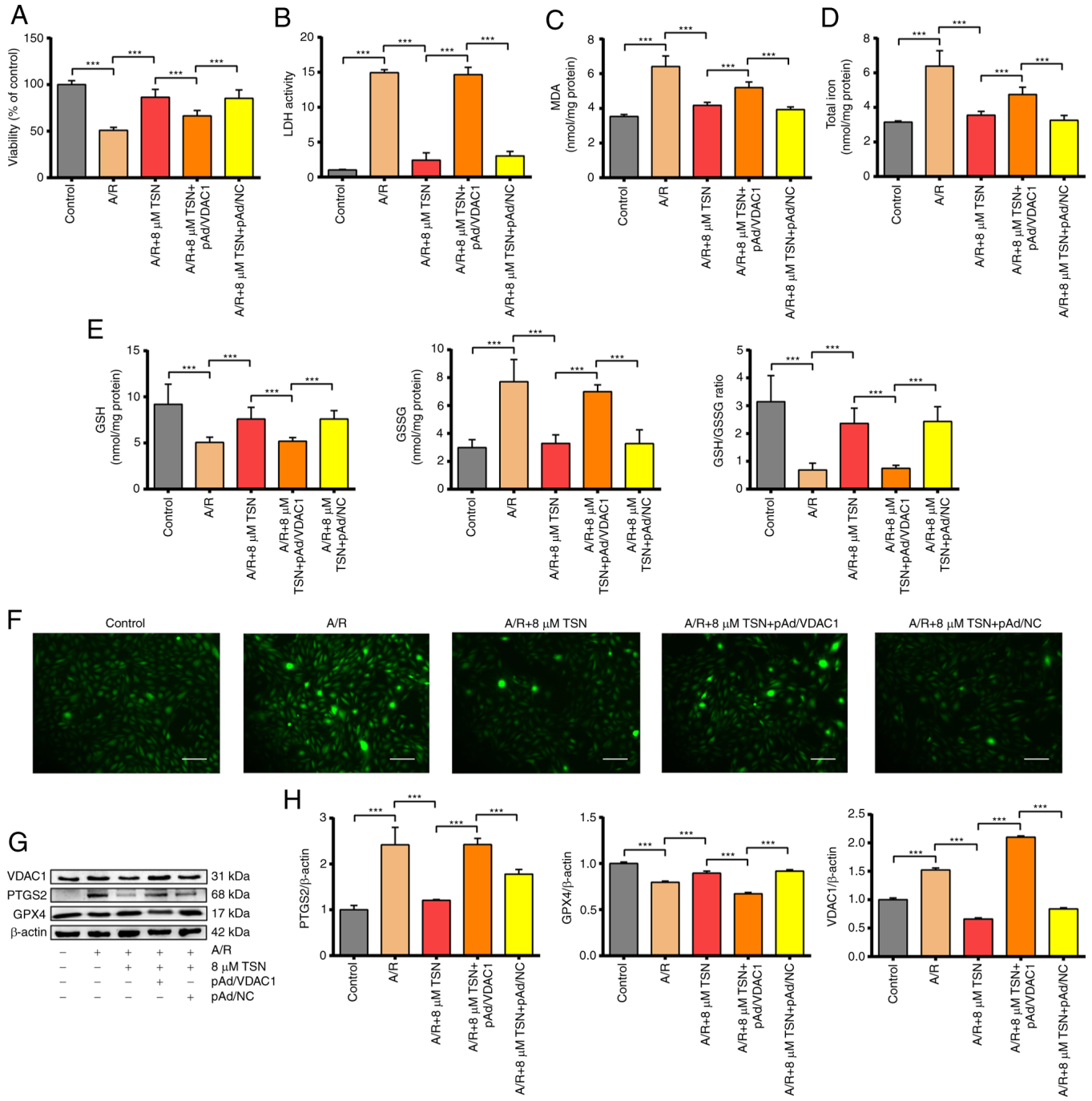

Figure 5. TSN inhibits ferroptosis of A/R-induced H9c2 cardiomyocytes by downregulating VDAC1. (A) Cell Counting Kit-8 detection of viability in A/R-induced cells after TSN, pAd/VDAC1 and pAd/NC pretreatment. (B) LDH, (C) MDA, (D) total iron, (E) GSH, GSSG, GSH/GSSG and (F) ROS were determined by quantitative kits in A/R-induced cells following TSN, pAd/VDAC1 and pAd/NC treatment (magnification, x200; scale bar, 50 μm). (G) Expression of (H) ferroptosis-associated proteins and VDAC1 were detected by western blot analysis in A/R-induced cells after TSN, pAd/VDAC1 and pAd/NC pretreatment. Data are expressed as the mean ± SD (n=3). ***P<0.05. TSN, tanshinone IIA; A/R, anoxia/reoxygenation; VDAC1, voltage-dependent anion channel 1; NC, negative control; LDH, lactate dehydrogenase; MDA, malondialdehyde; GSH, Glutathione; GSSG, Glutathione disulfide; ROS, reactive oxygen species; PTGS2, Prostaglandin endoperoxide synthase 2; GPX4, Glutathione peroxidase 4.

decreased the cell viability and increased the level of LDH activity, while pretreatment with TSN inhibited the injury induced by A/R (Fig. 5A and B). However, the protective effect of TSN was significantly eliminated by pAd/VDAC1, whereas pAd/NC could not abolish the protective effect of TSN. Thus, TSN might regulate VDAC1 to protect H9c2 cardiomyocytes against A/R injury. It was hypothesized that pretreatment with TSN could inhibit ferroptosis associated with IRI by downregulating VDAC1. Levels of MDA, total iron, intracellular ROS, GSH and GSSG were determined in H9c2 cardiomyocytes. Compared with the control group, the levels of MDA, total iron, intracellular ROS and GSSG were significantly increased in H9c2 cells after A/R injury and GSH and the GSH/GSSG ratio were significantly decreased. However, pretreatment with TSN could reverse the effects of A/R and pAd/VDAC1 prevented this reversion (Fig. 5C-F).

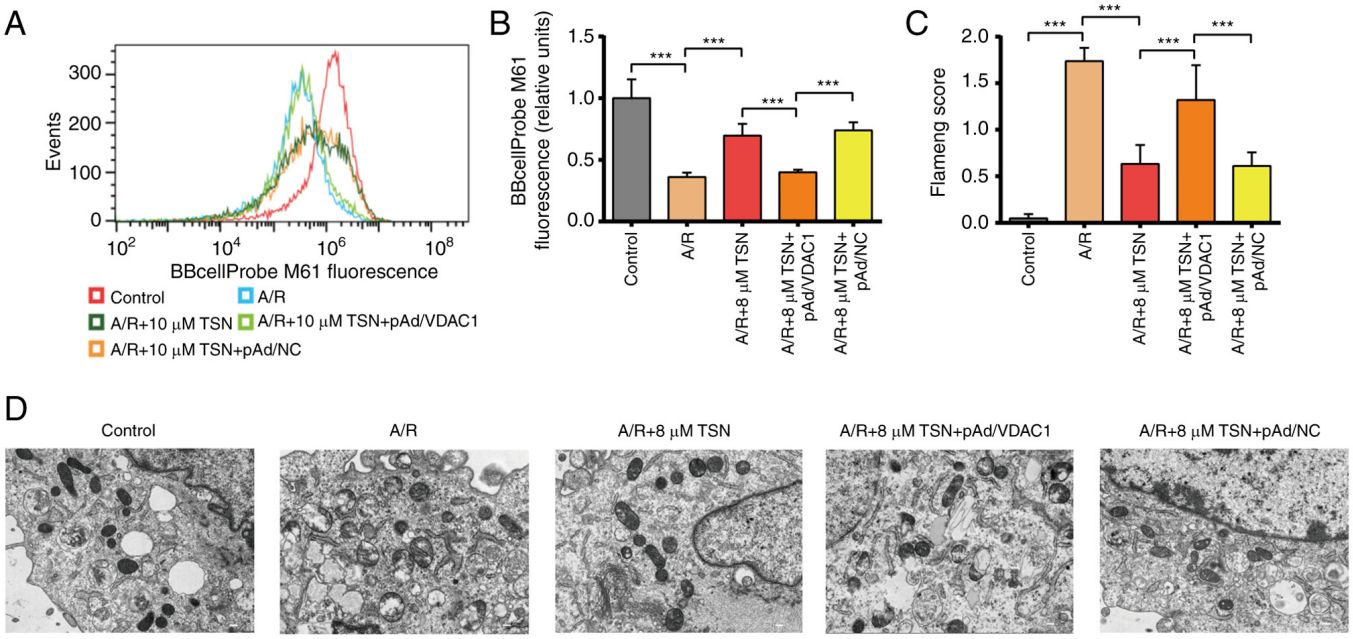

Figure 6. TSN improves mitochondrial function and integrity in H9c2 cardiomyocytes exposed to A/R by downregulating VDAC1. (A) Fluorescent probe BBcellProbe M61 indicating mPTP opening was detected by flow cytometry with the FL1-A: B525-FITC channel. (B) mPTP flow cytometry. (C) Flameng score and (D) transmission electron microscopy of H9c2 cells (magnification, x8,000; scale bar, 2 μm). Data are expressed as the mean ± SD (n=3). ***P<0.05. TSN, tanshinone IIA; A/R, Anoxia/reoxygenation; VDAC1, Voltage-dependent anion channel 1; mPTP, Mitochondrial permeability transition pore; NC, negative control.

In addition, ferroptosis-associated proteins (PTGS2 and GPX4) and VDAC1 were also determined *in vitro* using western blot analysis; A/R injury remarkably increased the level of PTGS2 and reduced the level of GPX4 compared with the control. Furthermore, pretreatment with TSN obviously inhibited the effects of A/R injury. In addition, pAd/VDAC1 significantly increased the protein levels of VDAC1. Pretreatment with TSN and pAd/VDAC1 significantly increased levels of PTGS2 and decreased GPX4 compared with pretreatment with TSN (Fig. 5G and H). TSN effectively inhibited ferroptosis in IRI mediated by VDAC1 and pAd/VDAC1 significantly prevented this inhibition.

Previous studies have demonstrated that VDAC1 is key for mPTP formation (16,17). Based on downregulated expression of VDAC1, the present study aimed to assess mitochondrial functional and morphological changes in TSN-treated H9c2 cardiomyocytes. TSN or pAd/NC pretreatment significantly decreased mPTP opening in H9c2 cardiomyocytes following A/R injury; pretreatment with pAd/VDAC1 reversed this effect (Fig. 6A and B). TEM indicated that the mitochondrial structure in A/R-treated H9c2 cells was notably distorted with fewer cristae, while the Flameng scores were significantly increased; these A/R-induced effects were prevented by TSN pretreatment, which was reversed by pAd/VDAC1 (Fig. 6C and D).

TSN inhibits apoptosis of A/R-induced H9c2 cardiomyocytes by downregulating. VDAC1 Previous studies have reported that apoptosis is a key form of cell death involved in IRI (2,38). Upon investigating the association between the protective effects of TSN on A/R injury and VDAC1, the present study demonstrated that protein levels of Bcl-2 and Bax, molecular markers of apoptosis (39), were notably decreased and significantly increased, respectively. Thus, Bcl-2/Bax ratio was significantly decreased in A/R-stimulated H9c2 cardiomyocytes compared with the control. However, pretreatment with TSN efficiently increased the Bcl-2/Bax ratio in H9c2 cardiomyocytes following A/R injury (Fig. 7A and B). Moreover, overexpression of VDAC1 significantly prevented the effects of TSN (Fig. 7A and B). Additionally, TSN suppressed the increased caspase-3 activity in H9c2 cardiomyocytes caused by A/R injury, which was reversed by pAd/VDAC1 (Fig. 7C).

Furthermore, to confirm that TSN inhibited apoptosis of A/R-induced H9c2 cardiomyocytes by adjusting VDAC1 (Fig. 8), MMP was determined by flow cytometry. Changes in MMP are characteristic of early apoptosis, reflect mitochondrial viability and can be detected by JC-1. In live cells with high levels of MMP, JC-1 accumulates in the mitochondrial matrix and produces red fluorescence, while in apoptotic and dead cells with low levels of MMP, JC-1 cannot aggregate in the mitochondrial matrix and only emits green fluorescence. Thus, red/green fluorescence ratio is used to assay loss of MMP (40). MMP levels were significantly increased in the A/R group compared with those in the control. Levels of MMP were significantly downregulated, whereas pretreatment with TSN significantly increased levels of MMP compared with A/R group. Furthermore, pAd/VDAC1 significantly prevented the protective effect of TSN on the A/R-induced decrease in MMP (Fig. 7D and F). Consistently, apoptotic rate was significantly induced in A/R group compared with that in control group and pretreatment with TSN significantly reversed the effects on apoptotic rate compared with the A/R group, whereas pAd/VDAC1 pretreatment abolished the protective effects of TSN (Fig. 7E and G).

These results showed that TSN attenuated apoptosis in A/R injury by downregulating VDAC1 (Fig. 8).

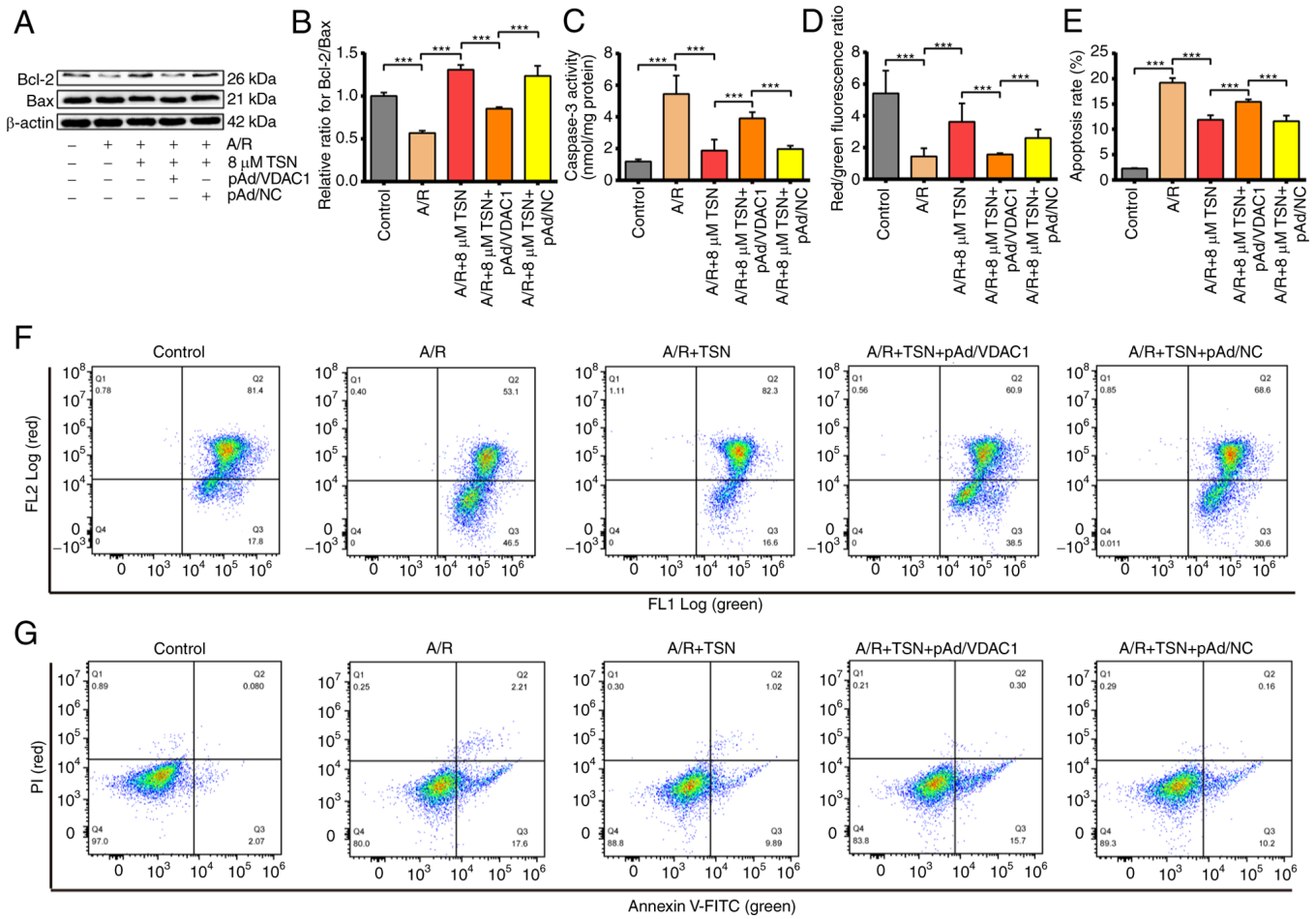

Figure 7. TSN inhibits apoptosis of A/R-induced H9c2 cardiomyocytes by downregulating VDAC1. (A) Expression of (B) apoptosis-associated proteins was detected by western blot analysis in A/R-induced cells following TSN, pAd/VDAC1 and pAd/NC pretreatment. (C) Caspase-3 activity was measured using a Caspase-3 kit in A/R-induced cells after TSN, pAd/VDAC1 and pAd/NC treatment. (D) MMP and (E) apoptosis were detected by flow cytometry. (F) MMP levels detected by JC-1 in H9c2 cells indicated by the red/green fluorescence ratio. (G) Apoptotic rate measured by Annexin V-FITC/PI flow cytometry. Data are expressed as the mean ± SD (n=3). ***P<0.05. TSN, Tanshinone IIA; A/R, Anoxia/reoxygenation; VDAC1, Voltage-dependent anion channel 1; NC, negative control; MMP, mitochondrial membrane potential.

Discussion

Although reoxygenation or reperfusion is an effective approach for AMI, it can lead to further serious tissue damage that accounts for expansion of the infarcted area and increased mortality in patients with AMI (1). Such injury is known as IRI (41). Previous studies have reported that the pathogenesis of IRI involves excessive ROS generation and inflammatory responses (42,43). The underlying molecular mechanisms and pathways of IRI are complicated and associated with multiple forms of regulated cell death, including pyroptosis, necroptosis, ferroptosis and apoptosis (44,45). Elucidating the underlying mechanisms is key in identifying therapeutic targets and drugs for IRI (46). The present study showed that in A/R-induced H9c2 cardiomyocytes, LDH activity increased and cell viability decreased significantly, suggesting that establishment of an *in vitro* model of IRI was successful.

Since the 'nutritional preconditioning' hypothesis was proposed, it has been the focus of many studies, which refers to the pretreatment of cells with nutrients before injuries (16,47). Pharmacological pretreatment is the most common approach to improve the outcome of numerous types of cardiovascular disease (48). For example, Puerarin preconditioning protects cardiomyocytes from sepsis-induced injury by inhibiting ferroptosis and apoptosis (49). It is hypothesized that TSN is also a candidate phytochemical. TSN, a bioactive natural product primarily extracted from the root of Danshen, is considered a nutriment and is used to produce soup or tea (9). However, it has also been used as a medicine in the US and Europe (10). Danshen has been used to treat stroke, skin disorders, spasms, and other ailments in Asian countries for hundreds of years (50,51). Additionally, pretreatment with TSN significantly alleviates apoptosis, oxidative stress and inflammatory responses to reduce cardiomyocyte death following IRI (52-54). Here, TSN pretreatment could effectively increase cell viability and reduced apoptotic rate and caspase-3 activity following A/R injury, which was similar to the protective effects of the apoptosis inhibitor Z-VAD and the ROS inhibitor NAC. However, TSN treatment at high concentration severely inhibits heart development and leads to cardiac toxicity (55). Here, TSN pretreatment effectively protected the myocardium against A/R injury. Cell viability following 32 μM TSN treatment was significantly decreased compared with other TSN doses in the A/R injury model, suggesting that

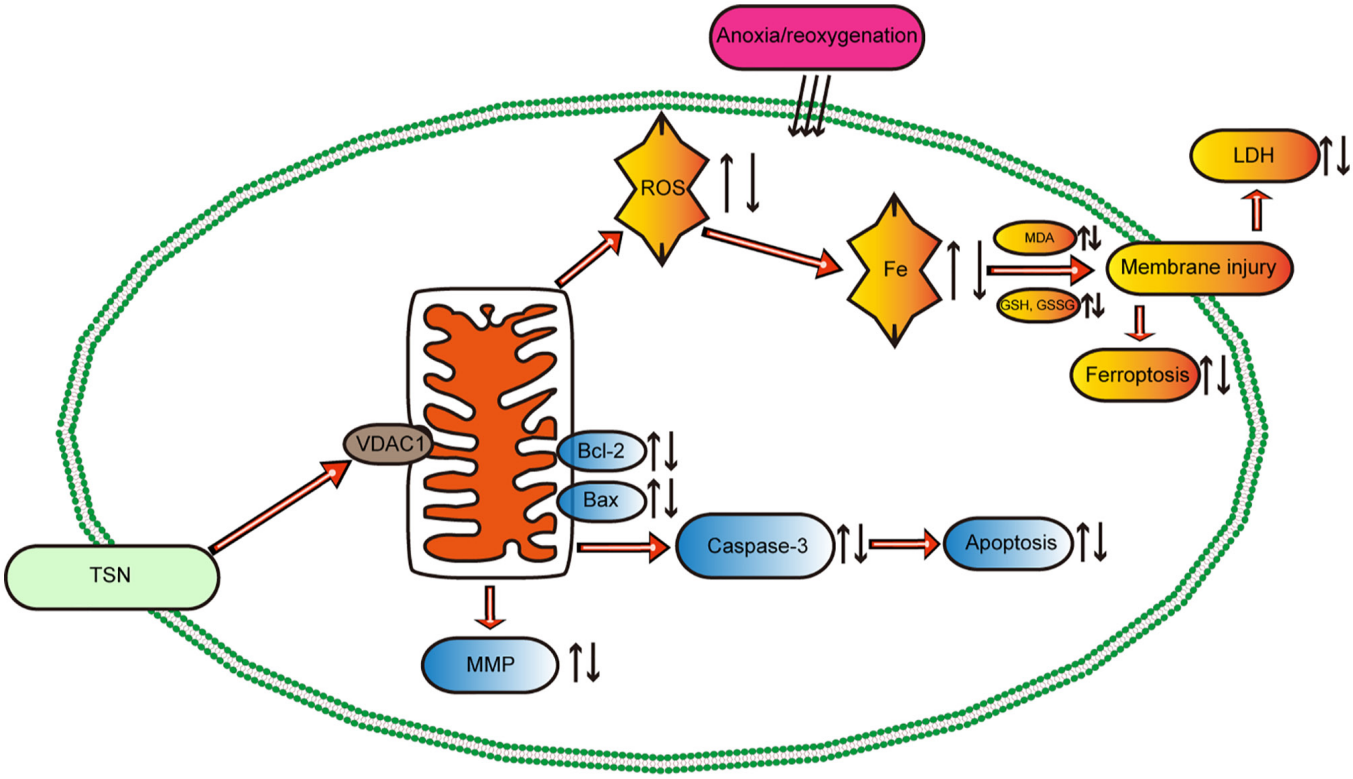

Figure 8. Potential mechanism of TSN in myocardial ischemia/reperfusion injury. TSN pretreatment upregulates the expression of VDAC1, thereby decreasing the accumulation of ROS and iron and abnormal lipid metabolism, maintaining mitochondrial function and protecting the myocardium against anoxia/reoxygenation-induced ferroptosis and apoptosis. TSN, tanshinone IIA; VDAC1, Voltage-dependent anion channel 1; ROS, reactive oxygen species; MDA, malondialdehyde; GSH, Glutathione; GSSG, Glutathione disulfide; LDH, lactate dehydrogenase; MMP, Mitochondrial membrane potential.

high concentrations of TSN could not attenuate A/R-induced cardiotoxicity.

Although a protective effect of TSN was identified, the underlying molecular mechanisms of action are unknown. Here, TSN and Fer-1 significantly downregulated A/R-induced VDAC1 upregulation and molecular docking simulation revealed the direct interaction between TSN and VDAC1. Furthermore, the potential association between VDAC1 and protection effect of TSN was explored. The effects of TSN were significantly reversed after the overexpression of VDAC1 using pAd/VDAC1. Therefore, it was concluded that VDAC1 was the target of TSN.

VDAC1 participates in the synthesis of mPTP, a key pore located in the outer membrane of the mitochondria and is involved in signal transduction and transport of metabolites (56,57). In numerous studies, it has been suggested that upregulated VDAC1 expression serves an important role in the pathological process of IRI, while overexpression of VDAC1 aggravates myocardial damage through the activation of mitochondrial apoptosis based on release of apoptotic factors (16,58). Here, VDAC1 overexpression prevented the protective effect of TSN against A/R injury. In addition, overexpression of VDAC1 could decrease the levels of MMP and apoptotic rate induced by TSN. Furthermore, overexpression of VDAC1 could open mPTP and inhibit the protective effect of TSN against mitochondrial damage during A/R injury. Therefore, TSN attenuates mitochondrial dysfunction and mitochondrial-related apoptosis induced by A/R injury via targeting VDAC1.

Apoptosis is a major form of cell death during IRI that involves various genes and signaling pathways, including Capase-3, Bax and Bcl-2 (59). Bcl-2 is an antiapoptotic gene and Bax is a proapoptotic gene, both of which belong to the Bcl-2 family, while apoptosis is mediated by the interaction between Bax and Bcl-2 (60). Previous studies have demonstrated that the apoptotic rate is associated with Bcl-2/Bax ratio; higher Bcl-2/Bax ratio represents a lower apoptotic rate (61,62). As a member of the caspase protein family, caspase-3 is involved in the activation and mediation of apoptosis as a key protease (63). The present study showed that TSN effectively increased the Bcl-2/Bax ratio and decreased Caspase-3 activity induced by A/R, while the protective effects of TSN pretreatment were prevented by overexpression of VDAC1. Taken together, TSN could prevent mitochondrial apoptosis following IRI by inhibiting upregulation of VDAC1.

Mitochondria play a key role in regulated cell death, including ferroptosis (iron-dependent) and apoptosis (caspase-regulated). VDAC1, as a key part of mPTP, is involved in ferroptosis during tissue damage and organ dysfunction induced by various types of disease such as cancer, Alzheimer's disease, and myocardial infraction (64,65). Ferroptosis has recently been identified as a key contributor to cell death during IRI but the underlying mechanisms of action of ferroptosis are yet to be elucidated (66). As a primary ferroptosis inhibitor, Fer-1 has been used in previous studies, while Fer-1 inhibits ferroptosis, which is primarily dependent on inhibiting lipid peroxidation (16,33). To the best of our knowledge, however, few studies have reported that the protective effects of Fer-1

are more effective and stable *in vivo* than *in vitro* (13,67). Thus, a more stable and effective ferroptosis inhibitor may further prevent tissue damage due to IRI. Previous studies have demonstrated that GPX4 and PTGS2 are key genes involved in the pathological process of ferroptosis and are regarded ferroptosis-specific markers (14,68). Therefore, in the present study, these two genes were selected as ferroptosis indicators. TSN significantly alleviated cell damage following A/R injury, which was similar to the protective effects of Fer-1. Additionally, VDAC1 overexpression effectively prevented the effects of TSN on the damage of cardiomyocytes resulting from A/R injury.

The major pathological process of ferroptosis is dependent on excess iron and lipoxygenase, which promote generation of ROS and other superoxides that cause lipid peroxidation via the Fenton reaction (69). Additionally, depletion of GSH and excess generation of GSSG lead to activation of ferroptosis (70). Increased total iron content, MDA (products of lipid peroxidation), ROS and GSSG are associated with ferroptosis (15). Following pretreatment with TSN or Fer-1, upregulation of genes related to ferroptosis and the levels of total iron, MDA, ROS and GSSG were significantly decreased, while GSH levels and the GSH/GSSG ratio were increased. However, the present study did not prove that TSN could exert a protective effect against A/R injury by inhibiting ferroptosis. Previous studies have reported that erastin treatment could effectively cause ferroptosis in H9c2 cardiomyocytes (71,72). The present study showed similar results that erastin treatment could remarkably increase levels of ferrous and total iron, lipid ROS and MDA and pretreatment with TSN could significantly prevent the effect of erastin on H9c2 cells, indicating that TSN could prevent ferroptosis. In summary, TSN remarkably attenuated cardiomyocyte injury by inhibiting ferroptosis during A/R. Overexpression of VDAC1 prevented the protective effects of TSN. Together, these results demonstrated that TSN effectively prevented ferroptosis following A/R injury via downregulation of VDAC1.

Here, only ferroptosis-specific inhibitors were used to investigate the molecular mechanisms of TSN's protection *in vitro*. To understand the underlying mechanisms of action, transgenic or knockout rat models or cells overexpressing VDAC1 and ferroptosis-associated genes are necessary and the protective effect of co-treatment with TSN and Fer-1 on A/R injury also requires further study. Additionally, although a direct interaction was predicted between TSN and VDAC1 using molecular docking, this should be validated using *ex vivo* pull-down assay. Finally, the ability of VDAC1 to transit between open and closed configurations is involved in the regulation of ferroptosis and apoptosis but was not confirmed in the present study (73).

The present study demonstrated that TSN protected cardiomyocytes from A/R injury by inhibiting ferroptosis and apoptosis. Additionally, protection of TSN was prevented by overexpression of VDAC1. VDAC1 and ferroptosis-related proteins play a vital role in the pathological process of IRI and clinical application of TSN deserves further study.

Acknowledgements

Not applicable.

Funding

The present study was supported by the Natural Science Foundation of Jiangxi, China (grant no. 20212BAB206021), Key Projects of Jiangxi Natural Science Foundation (grant no. 20224ACB206002), National Natural Science Foundation of China (grant nos. 81960059 and 82160073) and Jiangxi Provincial Natural Science Foundation (grant no. 20232BAB206009).

Availability of data and materials

The datasets used and/or analyzed during the current study are available from the corresponding author on reasonable request.

Authors' contributions

HH, SQ-L and JC-L conceived and designed the study. TH, HX-Z, HH, SQ-L and SY-L performed cell experiments and data analysis and interpretation. YR-W, YM-Q and YY performed cell experiments. All authors wrote the manuscript. All authors have read and approved the final manuscript. HH and SQ-L revised the manuscript. HH and SQ-L confirm the authenticity of all the raw data.

Ethics approval and consent to participate

Not applicable.

Patient consent for publication

Not applicable.

Competing interests

The authors declare that they have no competing interests.

References

1. Davidson SM, Ferdinandy P, Andreadou I, Bøtker HE, Heusch G, Ibáñez B, Ovize M, Schulz R, Yellon DM, Hausenloy DJ, *et al*: Multitarget strategies to reduce myocardial ischemia/reperfusion injury: JACC review topic of the week. J Am Coll Cardiol 73: 89-99, 2019.
2. Hausenloy DJ, Bøtker HE, Ferdinandy P, Heusch G, Ng GA, Redington A and Garcia-Dorado D: Cardiac innervation in acute myocardial ischaemia/reperfusion injury and cardioprotection. Cardiovasc Res 115: 1167-1177, 2019.
3. Lee JR, Park BW, Park JH, Lim S, Kwon SP, Hwang JW, Kim H, Park HJ and Kim BS: Local delivery of a senolytic drug in ischemia and reperfusion-injured heart attenuates cardiac remodeling and restores impaired cardiac function. Acta Biomater 135: 520-533, 2021.
4. Gumpper-Fedus K, Park KH, Ma H, Zhou X, Bian Z, Krishnamurthy K, Sermersheim M, Zhou J, Tan T, Li L, *et al*: MG53 preserves mitochondrial integrity of cardiomyocytes during ischemia reperfusion-induced oxidative stress. Redox Biol 54: 102357, 2022.
5. Ren D, Quan N, Fedorova J, Zhang J, He Z and Li J: Sestrin2 modulates cardiac inflammatory response through maintaining redox homeostasis during ischemia and reperfusion. Redox Biol 34: 101556, 2020.
6. Duan W, Yang Y, Yan J, Yu S, Liu J, Zhou J, Zhang J, Jin Z and Yi D: The effects of curcumin post-treatment against myocardial ischemia and reperfusion by activation of the JAK2/STAT3 signaling pathway. Basic Res Cardiol 107: 263, 2012.

7. LLi ZM, Xu SW and Liu PQ: Salvia miltiorrhizaBurge (Danshen): A golden herbal medicine in cardiovascular therapeutics. Acta Pharmacol Sin 39: 802-824, 2018.
8. Zhang X, Ma Z, Liang Q, Tang X, Hu D, Liu C, Tan H, Xiao C, Zhang B, Wang Y and Gao Y: Tanshinone IIA exerts protective effects in a LCA-induced cholestatic liver model associated with participation of pregnane X receptor. J Ethnopharmacol 164: 357-367, 2015.
9. Luo J, Song W, Yang G, Xu H and Chen K: Compound Danshen (Salvia miltiorrhiza) dripping pill for coronary heart disease: An overview of systematic reviews. Am J Chin Med 43: 25-43, 2015.
10. Shang Q, Xu H and Huang L: Tanshinone IIA: A promising natural cardioprotective agent. Evid Based Complement Alternat Med 2012: 716459, 2012.
11. Li Q, Shen L, Wang Z, Jiang HP and Liu LX: Tanshinone IIA protects against myocardial ischemia reperfusion injury by activating the PI3K/Akt/mTOR signaling pathway. Biomed Pharmacother 84: 106-114, 2016.
12. Xiao H, Zhang M, Wu H, Wu J, Hu X, Pei X, Li D, Zhao L, Hua Q, Meng B, *et al*: CIRKIL exacerbates cardiac ischemia/reperfusion injury by interacting with Ku70. Circ Res 130: e3-e17, 2022.
13. Zhao WK, Zhou Y, Xu TT and Wu Q: Ferroptosis: Opportunities and challenges in myocardial ischemia-reperfusion injury. Oxid Med Cell Longev 2021, 9929687, 2021,
14. Li J, Cao F, Yin HL, Huang ZJ, Lin ZT, Mao N, Sun B and Wang G: Ferroptosis: Past, present and future. Cell Death Dis 11: 88, 2020.
15. Chen X, Kang R, Kroemer G and Tang D: Ferroptosis in infection, inflammation, and immunity. J Exp Med 218: e20210518, 2021.
16. Feng Y, Madungwe NB, Imam Aliagan AD, Tombo N and Bopassa JC: Liproxstatin-1 protects the mouse myocardium against ischemia/reperfusion injury by decreasing VDAC1 levels and restoring GPX4 levels. Biochem Biophys Res Commun 520: 606-611, 2019.
17. He H, Wang L, Qiao Y, Zhou Q, Yang B, Yin L, Yin D and He M: Vinegar/Tetramethylpyrazine Induces Nutritional Preconditioning Protecting the Myocardium Mediated by VDAC1. Oxid Med Cell Longev 2021: 6670088, 2021.
18. Lin D, Cui B, Ren J and Ma J: Regulation of VDAC1 contributes to the cardioprotective effects of penehyclidine hydrochloride during myocardial ischemia/reperfusion. Exp Cell Res 367: 257-263, 2018.
19. Pooja S, Pushpanathan M, Gunasekaran P and Rajendhran J: Endocytosis-Mediated Invasion and Pathogenicity of Streptococcus agalactiae in Rat Cardiomyocyte (H9C2). PLoS One 10: e0139733, 2015.
20. Wang L, Lai S, Zou H, Zhou X, Wan Q, Luo Y, Wu Q, Wan L, Liu J and Huang H: Ischemic preconditioning/ischemic postconditioning alleviates anoxia/reoxygenation injury via the Notch1/Hes1/VDAC1 axis. J Biochem Mol Toxicol 36: e23199, 2022.
21. Zhou XL, Wu X, Xu QR, Zhu RR, Xu H, Li YY, Liu S, Huang H, Xu X, Wan L, *et al*: Notch1 provides myocardial protection by improving mitochondrial quality control. J Cell Physiol 234: 11835-11841, 2019.
22. Sayers EW, Beck J, Bolton EE, Bourexis D, Brister JR, Canese K, Comeau DC, Funk K, Kim S, Klimke W, *et al*: Database resources of the National Center for biotechnology information. Nucleic Acids Res 49: D10-D17, 2021.
23. Karimi F, Hamidian Y, Behrouzifar F, Mostafazadeh R, Ghorbani-HasanSaraei A, Alizadeh M, Mortazavi SM, Janbazi M and Naderi Asrami P: An applicable method for extraction of whole seeds protein and its determination through Bradford's method. Food Chem Toxicol 164: 113053, 2022.
24. Yoshida Y, Shimakawa S, Itoh N and Niki E: Action of DCFH and BODIPY as a probe for radical oxidation in hydrophilic and lipophilic domain. Free Radic Res 37: 861-872, 2003.
25. Flameng W, Borgers M, Daenen W and Stalpaert G: Ultrastructural and cytochemical correlates of myocardial protection by cardiac hypothermia in man. J Thorac Cardiovasc Sur 79: 413-424, 1980.
26. Liu X, Shi Y, Deng Y and Dai R: Using molecular docking analysis to discovery *Dregea sinensis* Hemsl. Potential mechanism of anticancer, antidepression, and immunoregulation. Pharmacogn Mag 13: 358-362, 2017.
27. UniProt Consortium: UniProt: A hub for protein information. Nucleic Acids Res 43: D204-D212, 2015.
28. Hähnke VD, Kim S and Bolton EE: PubChem chemical structure standardization. J Cheminform 10: 36, 2018.
29. Peng Y, Wang L, Zhang Z, He X, Fan Q, Cheng X, Qiao Y, Huang H, Lai S, Wan Q, *et al*: Puerarin activates adaptive autophagy and protects the myocardium against doxorubicin-induced cardiotoxicity via the 14-3-3γ/PKCε pathway. Biomed Pharmacother 153: 113403, 2022.
30. Van der Paal J, Neyts EC, Verlackt CCW and Bogaerts A: Effect of lipid peroxidation on membrane permeability of cancer and normal cells subjected to oxidative stress. Chem Sci 7: 489-498, 2016.
31. Camaschella C, Nai A and Silvestri L: Iron metabolism and iron disorders revisited in the hepcidin era. Haematologica 105: 260-272, 2020.
32. Dixon SJ, Lemberg KM, Lamprecht MR, Skouta R, Zaitsev EM, Gleason CE, Patel DN, Bauer AJ, Cantley AM, Yang WS, *et al*: Ferroptosis: An iron-dependent form of nonapoptotic cell death. Cell 149: 1060-1072, 2012.
33. Fang X, Wang H, Han D, Xie E, Yang X, Wei J, Gu S, Gao F, Zhu N, Yin X, *et al*: Ferroptosis as a target for protection against cardiomyopathy. Proc Natl Acad Sci USA 116: 2672-2680, 2019.
34. Zhao T, Wu W, Sui L, Huang Q, Nan Y, Liu J and Ai K: Reactive oxygen species-based nanomaterials for the treatment of myocardial ischemia reperfusion injuries. Bioact Mater 7: 47-72, 2022.
35. Zhang Z, Dalan R, Hu Z, Wang JW, Chew NW, Poh KK, Tan RS, Soong TW, Dai Y, Ye L and Chen X: Reactive oxygen species scavenging nanomedicine for the treatment of ischemic heart disease. Adv Mater 34: e2202169, 2022.
36. Zhou T, Wang Z, Guo M, Zhang K, Geng L, Mao A, Yang Y and Yu F: Puerarin induces mouse mesenteric vasodilation and ameliorates hypertension involving endothelial TRPV4 channels. Food Funct 11: 10137-10148, 2020.
37. Li T, Guo R, Zong Q and Ling G: Application of molecular docking in elaborating molecular mechanisms and interactions of supramolecular cyclodextrin. Carbohydr Polym 276: 118644, 2022.
38. Del Re DP, Amgalan D, Linkermann A, Liu Q and Kitsis RN: Fundamental mechanisms of regulated cell death and implications for heart disease. Physiol Rev 99: 1765-1817, 2019.
39. Ye J, Huang Y, Que B, Chang C, Liu W, Hu H, Liu L, Shi Y, Wang Y, Wang M, *et al*: Interleukin-12p35 knock out aggravates doxorubicin-induced cardiac injury and dysfunction by aggravating the inflammatory response, oxidative stress, apoptosis and autophagy in mice. EBioMedicine 35: 29-39, 2018.
40. He H, Zhou Y, Huang J, Wu Z, Liao Z, Liu D, Yin D and He M: Capsaicin protects cardiomyocytes against anoxia/reoxygenation injury via preventing mitochondrial dysfunction mediated by SIRT1. Oxid Med Cell Longev 2017: 1035702, 2017.
41. Lu M, Jia M, Wang Q, Guo Y, Li C, Ren B, Qian F and Wu J: The electrogenic sodium bicarbonate cotransporter and its roles in the myocardial ischemia-reperfusion induced cardiac diseases. Life Sci 270: 119153, 2021.
42. Ren D, Quan N, Fedorova J, Zhang J, He Z and Li J: Sestrin2 modulates cardiac inflammatory response through maintaining redox homeostasis during ischemia and reperfusion. Redox Biol 34: 101556, 2020.
43. Wang H, Zheng B, Che K, Han X, Li L, Wang H, Liu Y, Shi J and Sun S: Protective effects of safranal on hypoxia/reoxygenation-induced injury in H9c2 cardiac myoblasts via the PI3K/AKT/GSK3β signaling pathway. Exp Ther Med 22: 1400, 2021.
44. Heusch G: Myocardial ischaemia-reperfusion injury and cardioprotection in perspective. Nat Rev Cardiol 17: 773-789, 2020.
45. Maslov LN, Popov SV, Naryzhnaya NV, Mukhomedzyanov AV, Kurbatov BK, Derkachev IA, Boshchenko AA, Khaliulin I, Prasad NR, Singh N, *et al*: The regulation of necroptosis and perspectives for the development of new drugs preventing ischemic/reperfusion of cardiac injury. Apoptosis 27: 697-719, 2022.
46. Ma W, Wei S, Zhang B and Li W: Molecular Mechanisms of cardiomyocyte death in drug-induced cardiotoxicity. Front Cell Dev Biol 8: 434, 2020.
47. Abdukeyum GG, Owen AJ and McLennan PL: Dietary (n-3) long-chain polyunsaturated fatty acids inhibit ischemia and reperfusion arrhythmias and infarction in rat heart not enhanced by ischemic preconditioning. J Nutr 138: 1902-1909, 2008.
48. Hausenloy DJ and Yellon DM: The therapeutic potential of ischemic conditioning: An update. Nat Rev Cardiol 8: 619-629, 2011.
49. Zhou B, Zhang J, Chen Y, Liu Y, Tang X, Xia P, Yu P and Yu S: Puerarin protects against sepsis-induced myocardial injury through AMPK-mediated ferroptosis signaling. Aging (Albany NY) 14: 3617-3632, 2022.
50. Cheng TO: Cardiovascular effects of Danshen. Int J Cardiol 121: 9-22, 2007.

51. Zhang Z, He H, Qiao Y, Huang J, Wu Z, Xu P, Yin D and He M: Tanshinone IIA pretreatment protects H9c2 cells against Anoxia/reoxygenation injury: Involvement of the translocation of Bcl-2 to mitochondria mediated by 14-3-3η. Oxid Med Cell Longev 2018: 3583921, 2018.
52. Feng J, Li S and Chen H: Tanshinone IIA inhibits myocardial remodeling induced by pressure overload via suppressing oxidative stress and inflammation: Possible role of silent information regulator 1. Eur J Pharmacol 791: 632-639, 2016.
53. Tong Y, Xu W, Han H, Chen Y, Yang J, Qiao H, Hong D, Wu Y and Zhou C: Tanshinone IIA increases recruitment of bone marrow mesenchymal stem cells to infarct region via up-regulating stromal cell-derived factor-1/CXC chemokine receptor 4 axis in a myocardial ischemia model. Phytomedicine 18: 443-450, 2011.
54. Chen L, Wei L, Yu Q, Shi H and Liu G: Tanshinone IIA alleviates hypoxia/reoxygenation induced cardiomyocyte injury via lncRNA AK003290/miR-124-5p signaling. BMC Mol Cell Biol 21: 20, 2020.
55. Wang T, Wang C, Wu Q, Zheng K, Chen J, Lan Y, Qin Y, Mei W and Wang B: Evaluation of Tanshinone IIA developmental toxicity in Zebrafish embryos. Molecules 22: 660, 2017.
56. Zhou H, Zhang Y, Hu S, Shi C, Zhu P, Ma Q, Jin Q, Cao F, Tian F and Chen Y: Melatonin protects cardiac microvasculature against ischemia/reperfusion injury via suppression of mitochondrial fission-VDAC1-HK2-mPTP-mitophagy axis. J Pineal Res 63: e12413, 2017.
57. Jiang L, Wang H, Chen G, Feng Y, Zou J, Liu M, Liu K, Wang N, Zhang H, Wang K and Xiao X: WDR26/MIP2 interacts with VDAC1 and regulates VDAC1 expression levels in H9c2 cells. Free Radic Biol Med 117: 58-65, 2018.
58. Liao Z, Liu D, Tang L, Yin D, Yin S, Lai S, Yao J and He M: Long-term oral resveratrol intake provides nutritional preconditioning against myocardial ischemia/reperfusion injury: Involvement of VDAC1 downregulation. Mol Nutr Food Res 59: 454-464, 2015.
59. Zhang Y, Yang X, Ge X and Zhang F: Puerarin attenuates neurological deficits via Bcl-2/Bax/cleaved caspase-3 and Sirt3/SOD2 apoptotic pathways in subarachnoid hemorrhage mice. Biomed Pharmacother 109: 726-733, 2019.
60. Nishikawa S, Tatsumi T, Shiraishi J, Matsunaga S, Takeda M, Mano A, Kobara M, Keira N, Okigaki M, Takahashi T and Matsubara H: Nicorandil regulates Bcl-2 family proteins and protects cardiac myocytes against hypoxia-induced apoptosis. J Mol Cell Cardiol 40: 510-519, 2006.
61. Misao J, Hayakawa Y, Ohno M, Kato S, Fujiwara T and Fujiwara H: Expression of bcl-2 protein, an inhibitor of apoptosis, and Bax, an accelerator of apoptosis, in ventricular myocytes of human hearts with myocardial infarction. Circulation 94: 1506-1512, 1996.
62. Zhang L, Wang YN, Ju JM, Shabanova A, Li Y, Fang RN, Sun JB, Guo YY, Jin TZ, Liu YY, *et al*: Mzb1 protects against myocardial infarction injury in mice via modulating mitochondrial function and alleviating inflammation. Acta Pharmacolo Sin 42: 691-700, 2021.
63. Liou CM, Tsai SC, Kuo CH, Ting H and Lee SD: Cardiac Fas-dependent and mitochondria-dependent apoptosis after chronic cocaine abuse. Int J Mol Sci 15: 5988-6001, 2014.
64. Niu B, Lei X, Xu Q, Ju Y, Xu D, Mao L, Li J, Zheng Y, Sun N, Zhang X, *et al*: Protecting mitochondria via inhibiting VDAC1 oligomerization alleviates ferroptosis in acetaminophen-induced acute liver injury. Cell Biol Toxicol 38: 505-530, 2022.
65. Nagakannan P, Islam MI, Karimi-Abdolrezaee S and Eftekharpour E: Inhibition of VDAC1 protects against glutamate-induced oxytosis and mitochondrial fragmentation in hippocampal HT22 cells. Cell Mol Neurobiol 39: 73-85, 2019.
66. Liu P, Feng Y, Li H, Chen X, Wang G, Xu S, Li Y and Zhao L: Ferrostatin-1 alleviates lipopolysaccharide-induced acute lung injury via inhibiting ferroptosis. Cell Mol Biol Lett 25: 10, 2020.
67. Miotto G, Rossetto M, Di Paolo ML, Orian L, Venerando R, Roveri A, Vučković AM, Bosello Travain V, Zaccarin M, Zennaro L, *et al*: Insight into the mechanism of ferroptosis inhibition by ferrostatin-1. Redox Biol 28: 101328, 2020.
68. Zhang Z, Guo M, Li Y, Shen M, Kong D, Shao J, Ding H, Tan S, Chen A, Zhang F and Zheng S: RNA-binding protein ZFP36/TTP protects against ferroptosis by regulating autophagy signaling pathway in hepatic stellate cells. Autophagy 16: 1482-1505, 2020.
69. He YJ, Liu XY, Xing L, Wan X, Chang X and Jiang HL: Fenton reaction-independent ferroptosis therapy via glutathione and iron redox couple sequentially triggered lipid peroxide generator. Biomaterials 241: 119911, 2020.
70. Fu C, Wu Y, Liu S, Luo C, Lu Y, Liu M, Wang L, Zhang Y and Liu X: Rehmannioside A improves cognitive impairment and alleviates ferroptosis via activating PI3K/AKT/Nrf2 and SLC7A11/GPX4 signaling pathway after ischemia. J Ethnopharmacol 289: 115021, 2022.
71. Li S, Lei Z, Yang X, Zhao M, Hou Y, Wang D, Tang S, Li J and Yu J: Propofol protects myocardium from ischemia/reperfusion injury by inhibiting ferroptosis through the AKT/p53 signaling pathway. Front Pharmacol 13: 841410, 2022.
72. Xu S, Wu B, Zhong B, Lin L, Ding Y, Jin X, Huang Z, Lin M, Wu H and Xu D: Naringenin alleviates myocardial ischemia/reperfusion injury by regulating the nuclear factor-erythroid factor 2-related factor 2 (Nrf2)/System xc-/glutathione peroxidase 4 (GPX4) axis to inhibit ferroptosis. Bioengineered 12: 10924-10934, 2021.
73. Vander Heiden MG, Chandel NS, Li XX, Schumacker PT, Colombini M and Thompson CB: Outer mitochondrial membrane permeability can regulate coupled respiration and cell survival. Proc Natl Acad Sci USA 97: 4666-4671, 2000.